

# Enthalpy–Entropy of Cation Association with the Acetate Anion in Water

Timir Hajari, Pritam Ganguly, and Nico F. A. van der Vegt\*

Center of Smart Interfaces, Technische Universität Darmstadt, 64287 Darmstadt, Germany

**S** Supporting Information

**ABSTRACT:** Negatively charged carboxylate and phosphate groups on biomolecules have different affinity for  $\text{Na}^+$  and  $\text{K}^+$  ions. We performed molecular simulations and studied the pair potential of mean force between monovalent cations and the carboxylate group of the acetate anion in aqueous solution at 298 K. The simulations indicate that a larger affinity of  $\text{Na}^+$  over  $\text{K}^+$  in the contact ion pair (CIP) state is of entropic origin with the CIP state becoming increasingly populated at higher temperature. Differences between the osmotic activities of these two ions are however governed by interactions with acetate in the solvent-shared ion pair (SIP) state as was previously shown (Hess, B.; van der Vegt, N. F. A. *Proc. Natl. Acad. Sci. U.S.A.* **2009**, *106*, 13296). SIP states with  $\text{Na}^+$  are slightly more stable than SIP states with  $\text{K}^+$ , resulting in a smaller osmotic activity of sodium. We discuss the different affinities of  $\text{Na}^+$  and  $\text{K}^+$  in the SIP state in terms of an enthalpy–entropy reinforcement mechanism which involves a water-mediated hydrogen-bonding interaction between the oppositely charged ions. SIP states are enthalpically favorable and become decreasingly populated at higher temperature.

## 1. INTRODUCTION

Oppositely charged ions attract. In a dielectric medium, such as liquid water, this attraction is attenuated with a factor of approximately 78 (the dielectric constant, 298 K) and is independent of the specific ions involved, provided that the distance between them is large. However at small distances, where the attraction becomes appreciable in comparison to the thermal energy  $k_{\text{B}}T$ , the effective ion–ion interaction depends on the ion types and on the balance of ion–ion, ion–water, and water–water interactions.<sup>1,2</sup> The potential corresponding to the mean force between two ions separated by a distance  $r$  exhibits multiple minima.<sup>3–14</sup> At small distances, the first minimum corresponds to the contact ion pair (CIP). The second minimum corresponds to the solvent-shared ion pair (SIP) and is located at a slightly larger distance where the hydration sheaths of the two ions share a common water molecule. A third minimum, the solvent-separated ion pair (2SIP), can further be identified at a distance where the ions are separated by two water molecules. The stabilities (energy minima) of the CIP, SIP, and 2SIP states depend on the ion type.

Ion pairing in water affects dynamic and thermodynamic properties of the electrolyte solution. It has been long known that activity and osmotic coefficients of aqueous electrolyte solutions follow ion-specific series upon varying the cations or anions in solution.<sup>15</sup> The salt activity coefficient of an aqueous alkali chloride solution decreases with increasing crystallographic radius of the cation ( $\text{Li}^+ > \text{Na}^+ > \text{K}^+ > \text{Rb}^+ > \text{Cs}^+$ ). Contrarily, an exactly reversed series applies to aqueous alkali acetate solutions, with activity coefficients that increase as the crystallographic radius of the cation increases ( $\text{Li}^+ < \text{Na}^+ < \text{K}^+ < \text{Rb}^+ < \text{Cs}^+$ ). A recent explanation provided for this reversal of the ion series has been based on molecular simulations where it was analyzed how the excess occupation of CIP and SIP states varies among the ion types.<sup>16</sup> Ion specific variations in the activity coefficient of alkali chloride solutions could be

correlated with the excess occupation of CIP states, while the corresponding variations for alkali acetates could instead be correlated with the excess occupation of SIP states. In SIP configurations, the cation–anion interaction is solvent-mediated and becomes stronger with decreasing cation radius. This picture (see Figure 1), in which the anion accepts a hydrogen

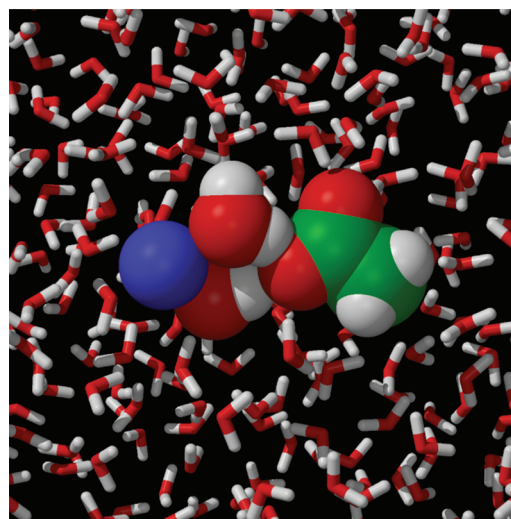


**Figure 1.** Solvent-shared ion pair between sodium (blue) and acetate in aqueous solution. The ions and the ion bridging water molecules are shown in van der Waals representation.

**Special Issue:** Wilfred F. van Gunsteren Festschrift

**Received:** January 31, 2012

**Published:** April 23, 2012

bond from water in the cation's first hydration shell, not only applies to carboxylate-based anions but also to dimethylphosphates, as was shown in subsequent work by Ganguly et al.<sup>17</sup>

Negatively charged carboxylate and phosphate groups on biomolecules interact differently with Na<sup>+</sup> and K<sup>+</sup> ions.<sup>18–23</sup>

The water-mediated interaction of sodium and potassium with these biological anions plays a key role in determining differences in their osmotic activities. Owing to its hydrogen-bonding nature, the expected, subtle differences between the interaction of sodium and potassium are sensitive to the thermodynamic conditions of temperature and pressure. In this paper, we study the effective interactions of three cations (Li<sup>+</sup>, Na<sup>+</sup>, K<sup>+</sup>) with the carboxylate group of the acetate ion. To this end, we consider the cation–anion pair potential of mean force (PMF) in a temperature range between 278 and 328 K. We discuss some thermodynamic aspects of ion pairing based on analyses of the enthalpy and entropy contributions to the PMFs.

## 2. SIMULATION DETAILS

Molecular dynamics (MD) simulations have been performed using the GROMACS package (version 4.0 and 4.5).<sup>24</sup> The nonbonded force field parameters for acetate and the cations are reported in References 16 and 17, the OPLS UA force-field<sup>25</sup> was used for the bonded parameters of acetate. The SPC/E model<sup>26</sup> was taken for water. Particle Mesh Ewald electrostatics<sup>27</sup> was used with a direct space cutoff of 1.0 nm and a grid spacing of 0.12 nm. For nonbonded van der Waals interactions, a 1.0 nm cutoff was used. All bond lengths for acetate molecules were kept constant using shake algorithm.<sup>28</sup> The temperature was kept constant using velocity rescale thermostat<sup>29</sup> with a relaxation time of 0.1 ps. The pressure was kept constant at 1 bar using the Berendsen barostat<sup>30</sup> with a relaxation time of 1 ps. All systems were equilibrated in a 10 ns NpT simulation. NpT trajectories of 90 ns were accumulated. The integration time step was 2 fs. All systems contained 5556 water molecules and 50 ion pairs, corresponding to a salt concentration of 0.5 m.

## 3. RESULTS

Figures 2–4 show cation–acetate radial distribution functions  $g(r)$  (RDFs) in the upper panels and the corresponding PMFs,  $\Delta G(r) = -RT \ln g(r)$ , in the lower panels at three different temperatures. The cation–acetate distances were computed with respect to the closest carboxylate oxygen, and the nonspherical volume for the normalization was taken into

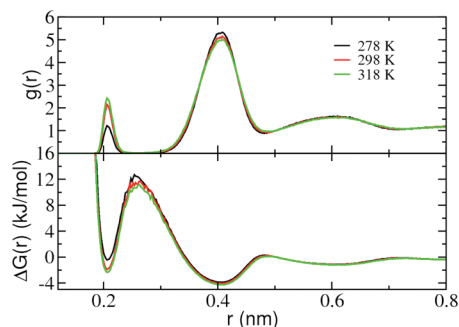


**Figure 2.** Radial distribution function between Li<sup>+</sup> and carboxyl oxygen in 0.5 m solution (upper panel). PMF between Li<sup>+</sup> and carboxyl oxygen in 0.5 m salt solution (lower panel).

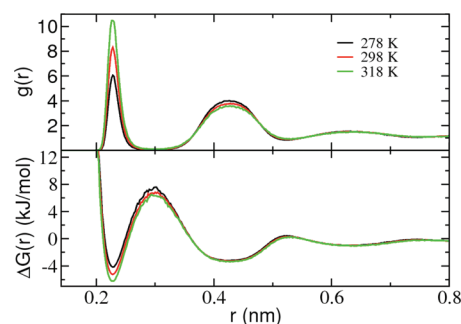


**Figure 3.** Radial distribution function between Na<sup>+</sup> and carboxyl oxygen in 0.5 m solution (upper panel). PMF between Na<sup>+</sup> and carboxyl oxygen in 0.5 m salt solution (lower panel).

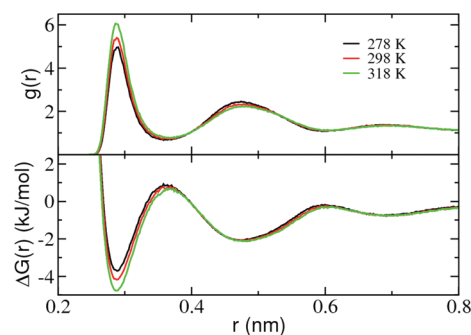


**Figure 4.** Radial distribution function between K<sup>+</sup> and carboxyl oxygen in 0.5 m solution (upper panel). PMF between K<sup>+</sup> and carboxyl oxygen in 0.5 m salt solution (lower panel).

account (for details we refer to the Supporting Information). The first peak in the RDF corresponds to the CIP, the second peak corresponds to the SIP. The stability ( $\Delta G$ ) of the CIP follows the order Na<sup>+</sup> > K<sup>+</sup> > Li<sup>+</sup>, while the stability of the SIP follows the order Li<sup>+</sup> > Na<sup>+</sup> > K<sup>+</sup>. Ion-specific thermodynamic properties are determined by the stability of SIPs.<sup>16</sup> With increasing temperature, we observe a larger CIP peak but a smaller SIP peak for all three cations. Hence, at higher temperature, the CIP population increases at the expense of the SIP population. Since the temperature derivative of  $g(r)$  is given by  $[\partial g(r)/\partial T]_p = g(r)\Delta H(r)/RT^2$ , we see that the enthalpy,  $\Delta H$ , in the CIP state is positive, while the enthalpy in the SIP state is negative (relative to large distances  $r \rightarrow \infty$ ). The lower panels in Figures 2–4 show the temperature dependence of the PMFs. Since the temperature derivative of the PMF,  $[\partial \Delta G(r)/\partial T]_p = -\Delta S(r)$ , provides the entropy,<sup>31</sup> it becomes clear that in the CIP state the entropy is positive for all cations. The same holds for the SIP states, but the temperature dependence, and therefore the entropy, is considerably smaller. We point out that in the simulations the entropies are calculated by taking finite temperature differences. The entropy calculated therefore assumes a constant heat capacity in the temperature range used for its calculation.

Before we analyze the free energies, enthalpies, and entropies in more detail, it is interesting to consider the predictions obtained with the primitive model, which views ions as point charges in a dielectric medium with dielectric permittivity  $\epsilon$ . The PMF of the primitive model is given by

$$\Delta G(r) = \frac{-1}{\epsilon r} \quad (1)$$

where we have ignored the constant factor  $e^2/4\pi\epsilon_0$ . Note that the primitive model in eq 1 is a free energy: the electrostatic screening results from averaging over solvent degrees of freedom at fixed ion distance  $r$  and is assumed to attenuate the Coulomb interaction between the two ions with a factor  $1/\epsilon$ . The dielectric permittivity of the solvent contains the information on the entropic changes of the solvent molecules involved in the charge–charge interaction. Taking the appropriate temperature derivatives provides the enthalpy and entropy:

$$\Delta H(r) = \Delta G(r) \left[ 1 + \frac{T}{\epsilon} \left( \frac{\partial \epsilon}{\partial T} \right) \right]$$

$$T\Delta S(r) = \Delta G(r) \left[ \frac{T}{\epsilon} \left( \frac{\partial \epsilon}{\partial T} \right) \right] \quad (2)$$

For liquid water at 298 K,<sup>32</sup>

$$\frac{T}{\epsilon} \left( \frac{\partial \epsilon}{\partial T} \right) = -1.36 \quad (3)$$

which shows that the primitive model predicts a positive change enthalpy change as well as a positive entropy change upon the approach of two oppositely charged ions in water, i.e., the polarization of the dielectric medium by the two ions contributes to a negative enthalpy and entropy but is reduced when the two ions are brought together.

Figure 5 shows the temperature dependence of the CIP free energies  $\Delta G_{\text{CIP}}$  of the systems containing  $\text{Li}^+$ ,  $\text{Na}^+$ , and  $\text{K}^+$ . The

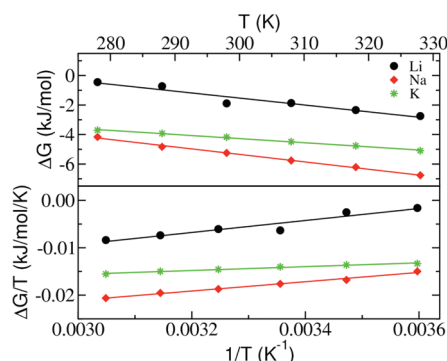


**Figure 5.** Temperature dependence of the CIP free energy minimum  $\Delta G_{\text{CIP}}$ . The slopes in the upper panel provide the CIP entropy  $-\Delta S_{\text{CIP}}$ , and the slopes in the lower panel provide the CIP enthalpy  $\Delta H_{\text{CIP}}$ .

free energies,  $\Delta G_{\text{CIP}}$ , enthalpies,  $\Delta H_{\text{CIP}}$ , and entropies,  $T\Delta S_{\text{CIP}}$ , obtained from the simulations are listed in Table 1 for  $T = 298$  K together with the predictions of the primitive model (values in parentheses). The CIP enthalpies and entropies are both positive, in agreement with the expectation based on the primitive model. Entropies  $T\Delta S_{\text{CIP}}$ , computed using the primitive model (eqs 1–3, using CIP and SIP distances  $r$  from the peak positions in Figures 2–4), are remarkably close to the values obtained from the simulations. The enthalpies  $\Delta H_{\text{CIP}}$  obtained from the simulations are however significantly larger (a factor of 2–4) than the values obtained with the primitive model, in particular for the strongly hydrated (kosmotropic)<sup>1,2,33</sup>  $\text{Li}^+$  and  $\text{Na}^+$  ions. Upon CIP formation, these ions release part of their hydration water, which contributes to a positive change in enthalpy and entropy.

**Table 1.** Thermodynamic Properties (units kJ/mol) of the CIP and SIP with Acetate (298 K, 1 bar)<sup>a</sup>

CIP state	$\Delta G_{\text{CIP}}$	$\Delta H_{\text{CIP}}$	$T\Delta S_{\text{CIP}}$
$\text{Li}^+$	$-1.4 \pm 0.2$ (−8.6)	$12.6 \pm 1.9$ (3.1)	$14.0 \pm 1.7$ (11.7)
$\text{Na}^+$	$-5.3 \pm 0.1$ (−7.8)	$9.8 \pm 0.9$ (2.8)	$15.1 \pm 0.8$ (10.6)
$\text{K}^+$	$-4.4 \pm 0.0$ (−6.2)	$4.0 \pm 0.2$ (2.2)	$8.4 \pm 0.2$ (8.4)
SIP state	$\Delta G_{\text{SIP}}$	$\Delta H_{\text{SIP}}$	$T\Delta S_{\text{SIP}}$
$\text{Li}^+$	$-4.0 \pm 0.01$ (−4.4)	$-1.1 \pm 0.1$ (1.6)	$2.9 \pm 0.1$ (6.0)
$\text{Na}^+$	$-3.3 \pm 0.03$ (−4.2)	$-1.8 \pm 0.2$ (1.5)	$1.5 \pm 0.2$ (5.7)
$\text{K}^+$	$-2.1 \pm 0.02$ (−3.7)	$-1.4 \pm 0.1$ (1.3)	$0.7 \pm 0.1$ (5.0)

<sup>a</sup>Statistical errors have been obtained by block averaging. The numbers in parentheses are the predictions of the primitive model (eqs 1–3).

Interestingly, the enthalpy and entropy changes in the CIP state are significantly smaller for the (chaotropic)  $\text{K}^+$  ion (Table 1), which is a weaker water binder.

Figure 6 shows the temperature dependence of the SIP free energies,  $\Delta G_{\text{SIP}}$ , of the systems containing  $\text{Li}^+$ ,  $\text{Na}^+$ , and  $\text{K}^+$ .

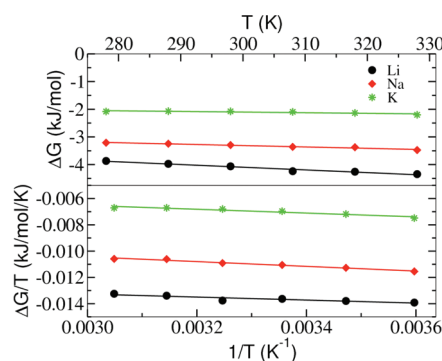


**Figure 6.** Temperature dependence of the SIP free energy minimum  $\Delta G_{\text{SIP}}$ . The slopes in the upper panel provide the SIP entropy  $-\Delta S_{\text{SIP}}$ , and the slopes in the lower panel provide the SIP enthalpy  $\Delta H_{\text{SIP}}$ .

The free energies,  $\Delta G_{\text{SIP}}$ , enthalpies,  $\Delta H_{\text{SIP}}$ , and entropies,  $T\Delta S_{\text{SIP}}$ , are listed in Table 1 for  $T = 298$  K. The temperature dependence of  $\Delta G_{\text{SIP}}$  is significantly weaker than the temperature dependence of  $\Delta G_{\text{CIP}}$ . While the entropies  $T\Delta S_{\text{SIP}}$  are all small and positive, the enthalpies  $\Delta H_{\text{SIP}}$  are all small and negative. This type of enthalpy–entropy reinforcement is not predicted by the primitive model and warrants further comment, in particular because the salt activities of this system owe their cation specificity from differences in SIP stability.<sup>16,17</sup> Interestingly, the entropies  $T\Delta S_{\text{SIP}}$  obtained from the simulations are significantly smaller than the corresponding entropies predicted by the primitive model (see Table 1). A possible explanation for this may be sought in a water-mediated interaction that stabilizes the SIP state. The water molecule shared between the cation and the carboxylate group of the anion coordinates the cation with its oxygen atom while donating a hydrogen bond to one of the carboxyl oxygen atoms (see Figure 1). This cation–anion bridging interaction via hydrogen-bonding decreases the enthalpy; the entropy tends to decrease too due to the ordering of the bridging water molecules. Fennell et al. observed orientationally constrained water molecules in SIP states of alkali halides.<sup>14</sup> Although these authors did not calculate the entropies of the different ion pair states, their results indicate that SIP states of alkali halides also have a low entropy. Interestingly, Baron et al.<sup>34</sup> reported two



examples of enthalpy dominated ion pairing for a model cavity–ligand system. In both cases described, enthalpy dominated ion pairing is solvent separated.<sup>34</sup>

Enthalpy–entropy compensation is a general property of weak intermolecular interactions,<sup>35–37</sup> which in SIP formation between monovalent cations and a carboxylate-based anion in water as studied here leads to lower enthalpies and entropies than expected based on simple electrostatic considerations. To investigate if the bridging water molecule is indeed configurationally confined compared to similar water molecules not hydrogen bonded to carboxylate, we considered the angle defined by the positions of the cation and the water oxygen and hydrogen atoms. Only those water molecules in the first hydration shell of the cation that donate a hydrogen bond to a carboxyl oxygen atom were considered in the analysis. The angle distribution functions are shown as solid lines in Figure 7.

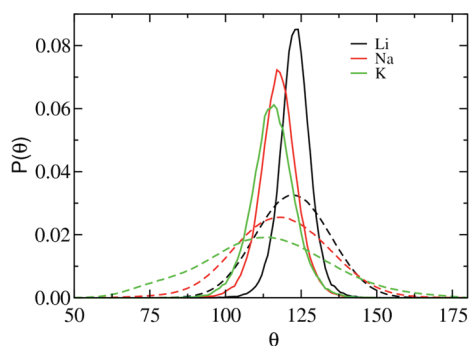


**Figure 7.** Distribution functions of the cation–oxygen(water)–hydrogen(water) angle for water molecules in the first hydration shell of the cation (298 K).  $\int_0^\pi P(\theta) d\theta = 1$ . The solid lines show the distribution functions for water molecules that are furthermore hydrogen bonded to the carboxyl oxygen in SIP configurations. The dashed lines show the distribution functions for water molecules in the cation first hydration shell but in the absence of the carboxylate group.

An angle of 125° corresponds to a water molecule that orients its dipole vector along the cation–oxygen(water) connecting vector. Similar angle distribution functions were calculated for cations in bulk water (in absence of an acetate ion), where, instead of hydrogen bonding with acetate, the cation's first shell hydration water molecule donates hydrogen bonds to the bulk. The corresponding distribution functions are shown as dashed lines in Figure 7. The comparison between the dashed and solid lines clearly indicates that bridging water molecules in SIP configurations sample a significantly narrower range of angles, therefore providing support for the idea that the water-mediated hydrogen-bonding interaction between the two ions lowers the water entropy. We further note that the widths of the distribution functions in Figure 7 decrease in the order  $K^+ > Na^+ > Li^+$ , which is also the order in which the cation–water interaction becomes stronger.

We finally examined the hydrogen-bond angle between the bridging water molecule and the acetate anion. The data are shown in Figure 8 (solid lines) and are compared with the acetate–water hydrogen bond angle distribution of 'free' acetate (dashed lines) far away from any cation. The comparison again shows that a smaller range of angles is sampled in the SIP state. Hydrogen bonds are slightly more bendable in the SIP state, as indicated by a small shift of the peaks to smaller angles in comparison to the free acetate case.

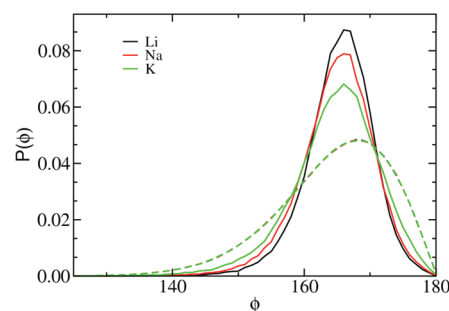


**Figure 8.** Distribution functions of the oxygen(carboxyl)–hydrogen(water)–oxygen(water) hydrogen-bond angle (298 K).  $\int_0^\pi P(\phi) d\phi = 1$ . The solid lines show the distribution functions for water molecules that furthermore belong to the first hydration shell of the cation in SIP configurations. The dashed lines show the distribution functions in absence of the cation.

#### 4. DISCUSSION AND CONCLUSIONS

Solvated ions are a common component of nearly all biological systems. In this work we have been interested in the interaction of monovalent cations with the negatively charged carboxylate group of the acetate anion. This anion serves as a model of negatively charged groups on biomolecules. There have been many studies that illustrate pronounced effects of dissolved, specific salts on properties, such as enzymatic activity, protein stability, and protein–protein interaction. Water plays an important, but ill-understood, role in these hydrophilic interactions, and the link to solution thermodynamic properties remains largely unexplored. Studies on the structure and thermodynamics of aqueous electrolyte solutions may potentially provide useful insights that advance our understanding of electrostatic interactions in biomolecular systems.

Salt activities and osmotic pressures of aqueous electrolyte solutions are ion specific. At high enough electrolyte concentrations, the osmotic pressures of NaCl and KCl solutions are different owing to different affinities of cation–anion pairing in these systems. The osmotic pressures of alkali chloride solutions thus depend on the choice of the cation. This dependence is uniquely determined by differences in the contact ion pairing propensities as was shown by Hess and van der Vegt,<sup>16</sup> who applied the thermodynamic solution theory of Kirkwood and Buff<sup>38</sup> to molecular dynamics simulation trajectories. Because Kirkwood–Buff theory provides an exact link between the solution thermodynamics and the solution structure (with the structure being expressed in terms of RDFs), our discussion of the solution thermodynamics can be limited to analyzing pair correlations only. Fennell et al.<sup>14</sup> computed various alkali–halide pair PMFs in aqueous solutions based on molecular dynamics simulations. These simulation studies<sup>14,16</sup> confirm Collins' law of matching water affinities,<sup>1,2</sup> which states that the relative affinities of ions in solution depend on the matching of cation and anion sizes: small pairs with small and large pairs with large, while small–large ion combinations should remain dissociated. Collins' law is based on enthalpic considerations, and entropy effects are assumed unimportant.

The appellations "chaotrope" and "kosmotrope" are sometimes used as synonyms of "large" and "small", respectively. Chaotropes are "structure breaking" ions, kosmotropes are "structure making" ions.<sup>33</sup> Among a plethora of quantities that can be used to characterize "structure", the ion–water and water–water RDFs provide one possible choice, which is

probably the most meaningful one because Kirkwood–Buff solution theory relates the RDFs to the solution thermodynamics. While certain aspects of the ion–water radial distribution function of chaotropic and kosmotropic ions can be correlated with single ion hydration entropies,<sup>39</sup> it was shown previously that differences in ion–water and water–water pair correlations in solutions with different cations do not explain the differences in the solution osmotic pressures.<sup>16,17</sup> Hence, ion-specific trends in the solution osmotic pressures of these systems can be explained by studying the ion–ion correlations only. These ion–ion correlations contain information on CIPs, SIPs, and 2SIPs, which can in principle be probed with dielectric relaxation spectroscopy. This promising experimental technique has had considerable success in measuring ion pairing.<sup>40–42</sup>

In this paper, we have reported molecular simulations and calculated ion pair PMFs to study the interaction of monovalent cations ( $\text{Li}^+$ ,  $\text{Na}^+$ ,  $\text{K}^+$ ) with the carboxylate group of the acetate anion in water. Previous simulations of this system<sup>16</sup> showed that cation–carboxylate CIPs and SIPs are stronger for  $\text{Na}^+$  than for  $\text{K}^+$ . It was furthermore shown that the resulting salt activity/osmotic coefficients are cation specific and follow the order  $\text{Li}^+ < \text{Na}^+ < \text{K}^+$ , exclusively owing to a decreasing stability of water-mediated SIPs in passing from  $\text{Li}^+$  to  $\text{K}^+$  within this series. The purpose of the present paper has been to characterize the thermodynamic properties of CIPs and SIPs in terms of their enthalpic and entropic stabilization. Because, also in this system, the ion–water and water–water correlations do not explain the ion specificity of the osmotic coefficients,<sup>16</sup> we have exclusively studied the cation–anion pair PMFs together with the contributions of the enthalpy and entropy. We find that for all three cations, the CIP and SIP states have positive entropy relative to the solvent-separated state at large ion separations. The magnitude of the entropy change follows the order  $\text{Na}^+ > \text{Li}^+ > \text{K}^+$  (CIP) and  $\text{Li}^+ > \text{Na}^+ > \text{K}^+$  (SIP). Ion pairing causes a significantly larger entropy gain for the strong water-binding (kosmotropic) cations  $\text{Li}^+$  and  $\text{Na}^+$  than for the weak water-binding (chaotropic)  $\text{K}^+$  ion. In the CIP state, positive entropies are compensated by a positive enthalpy. This enthalpy–entropy compensation phenomenon results in increased stability ( $\Delta G$ ) and population of CIP configurations with increasing temperature above 298 K. In the SIP state, enthalpy–entropy reinforcement stabilizes the SIP configuration, but its population decreases with increasing temperature above 298 K. The favorable enthalpy of SIP configurations results from a hydrogen-bonding interaction mechanism in which water molecules in the first shell of a cation donate hydrogen bonds to one of the carboxylate oxygens.

It is interesting to point out that surface salt bridges on hyperthermophilic proteins are believed to contribute to protein stability at elevated temperatures by a mechanism which is similar to the one described here.<sup>43,44</sup> At room temperature, desolvation of the charged side chains penalizes salt bridge formation and leads to little contribution of salt bridges to protein stability. At elevated temperatures, reduced solvation removes this penalty causing a favorable change in the intraprotein Coulomb energy due to the tightening of salt bridges.<sup>44</sup> The results presented in this work pertain to simple, spherical alkali cations. It would be interesting to further study ammonium or guanidinium-based cations in order to shed further light on the role of hydration and solvent entropy in salt bridge formation at different temperatures.

## ■ ASSOCIATED CONTENT

### § Supporting Information

The normalization of the cation–oxygen(carboxylate) radial distribution functions with a nonspherical volume is described. This information is available free of charge via the Internet at <http://pubs.acs.org>.

## ■ AUTHOR INFORMATION

### Corresponding Author

\*E-mail: [vandervegt@csi.tu-darmstadt.de](mailto:vandervegt@csi.tu-darmstadt.de)

### Notes

The authors declare no competing financial interest.

## ■ ACKNOWLEDGMENTS

N.F.A.v.d.V. is indebted to Wilfred van Gunsteren for encouragement and support at a decisive stage of his career and for introducing him to the field of entropy calculations.

## ■ DEDICATION

This work is dedicated to Wilfred van Gunsteren on the occasion of his 65th birthday.

## ■ REFERENCES

- (1) Collins, K. D. *Biophys. J.* **1997**, 72, 65.
- (2) Collins, K. D. *Methods* **2004**, 34, 300.
- (3) Neilson, G. W.; Enderby, J. E. *Proc. R. Soc. London, Ser. A* **1983**, 390, 353.
- (4) Patey, G. N.; Valleau, J. P. *J. Chem. Phys.* **1975**, 63, 2334.
- (5) Mezei, M.; Beveridge, D. L. *J. Chem. Phys.* **1981**, 74, 6902.
- (6) Pettitt, B. M.; Rossky, P. J. *J. Chem. Phys.* **1986**, 84, 5836.
- (7) Dang, L. X. *J. Chem. Phys.* **1992**, 97, 1919.
- (8) Chen, S. W.; Rossky, P. J. *J. Phys. Chem.* **1993**, 97, 6078.
- (9) Pratt, L. R.; Hummer, G.; Garcia, A. E. *Biophys. Chem.* **1994**, 51, 147.
- (10) Koneshan, S.; Rasaiah, J. C. *J. Chem. Phys.* **2000**, 113, 8125.
- (11) Bergdorf, M.; Peter, C.; Hünenberger, P. H. *J. Chem. Phys.* **2003**, 119, 9129.
- (12) Hess, B.; Holm, C.; van der Vegt, N. F. A. *Phys. Rev. Lett.* **2006**, 96, 147801.
- (13) Hess, B.; Holm, C.; van der Vegt, N. F. A. *J. Chem. Phys.* **2006**, 124, 164509.
- (14) Fennell, C. J.; Bizjak, A.; Vlachy, V.; Dill, K. A. *J. Phys. Chem. B* **2009**, 113, 6782.
- (15) Robinson, R. A.; Stokes, R. H. *Electrolyte Solutions*, 2nd ed.; Dover Publications: Mineola, NY, 2002.
- (16) Hess, B.; van der Vegt, N. F. A. *Proc. Natl. Acad. Sci. U.S.A.* **2009**, 106, 13296.
- (17) Ganguly, P.; Schravendijk, P.; Hess, B.; van der Vegt, N. F. A. *J. Phys. Chem. B* **2011**, 115, 3734.
- (18) Vrbka, L.; Vondrasek, J.; Jagoda-Cwiklik, B.; Vacha, R.; Jungwirth, P. *Proc. Natl. Acad. Sci. U.S.A.* **2006**, 103, 15440.
- (19) Savelyev, A.; Papoian, G. A. *J. Am. Chem. Soc.* **2006**, 128, 14506.
- (20) Jagoda-Cwiklik, B.; Vacha, R.; Lund, M.; Srebro, M.; Jungwirth, P. *J. Phys. Chem. B* **2007**, 111, 14077.
- (21) Aziz, E. F.; et al. *J. Phys. Chem. B* **2008**, 112, 12567.
- (22) Uejio, J. S.; Schwartz, C. P.; Duffin, A. M.; Drisdell, W. S.; Cohen, R. C.; Saykally, R. J. *Proc. Natl. Acad. Sci. U.S.A.* **2008**, 105, 6809.
- (23) Savelyev, A.; Papoian, G. A. *J. Phys. Chem. B* **2008**, 112, 9135.
- (24) Hess, B.; Kutzner, C.; van der Spoel, D.; Lindahl, E. *J. Chem. Theory Comput.* **2008**, 4, 435.
- (25) Jorgensen, W. L.; Maxwell, D. S.; Tirado-Rives, J. *J. Am. Chem. Soc.* **1996**, 118, 11236.
- (26) Berendsen, H. J. C.; Grigera, J. R.; Straatsma, T. P. *J. Phys. Chem.* **1987**, 91, 6269.

- (27) Essmann, U.; Perera, L.; Berkowitz, M. L.; Darden, T.; Lee, H.; Pedersen, L. G. *J. Chem. Phys.* **1995**, *103*, 8577.
- (28) Ryckaert, J. P.; Ciccotti, G.; Berendsen, H. J. C. *J. Comput. Phys.* **1977**, *23*, 327.
- (29) Bussi, G.; Donadio, D.; Parrinello, M. *J. Chem. Phys.* **2007**, *126*, 014101.
- (30) Berendsen, H. J. C.; Postma, J. P. M.; van Gunsteren, W. F.; DiNola, A.; Haak, J. R. *J. Chem. Phys.* **1984**, *81*, 3684.
- (31) Smith, D. E.; Zhang, L.; Haymet, A. D. J. *J. Am. Chem. Soc.* **1992**, *114*, 5875.
- (32) Israelachvili, J. N. *Intermolecular and Surface Forces*, 3rd ed., Academic Press: Burlington, MA, 2011.
- (33) Marcus, Y. *Chem. Rev.* **2009**, *109*, 1346.
- (34) Baron, R.; Setny, P.; McCammon, J. A. *J. Am. Chem. Soc.* **2010**, *132*, 12091.
- (35) Dunitz, J. *Chem. Biol.* **1995**, *2*, 709.
- (36) van der Vegt, N. F. A.; van Gunsteren, W. F. *J. Phys. Chem. B* **2004**, *108*, 1056.
- (37) van Gunsteren, W. F.; Bakowies, D.; Baron, R.; Chandrasekhar, I.; Christen, M.; Daura, X.; Gee, P.; Geerke, D. P.; Glättli, A.; Hünenberger, P. H.; Kastenholz, M. A.; Oostenbrink, C.; Schenk, M.; Trzesniak, D.; van der Vegt, N. F. A.; Yu, H. B. *Angew. Chem., Int. Ed.* **2006**, *45*, 4064.
- (38) Kirkwood, J. G.; Buff, F. P. *J. Chem. Phys.* **1951**, *19*, 774.
- (39) Lynden-Bell, R. M.; Rasaiah, J. C. *J. Chem. Phys.* **1997**, *107*, 1981.
- (40) Buchner, R.; Chen, T.; Hefter, G. *J. Phys. Chem. B* **2004**, *108*, 2365.
- (41) Wachter, W.; Kunz, W.; Buchner, R.; Hefter, G. *J. Phys. Chem. A* **2005**, *109*, 8675.
- (42) Marcus, Y.; Hefter, G. *Chem. Rev.* **2006**, *106*, 4585.
- (43) Elcock, A. H. *J. Mol. Biol.* **1998**, *284*, 489.
- (44) de Bakker, P. I.; Hünenberger, P. H.; McCammon, J. A. *J. Mol. Biol.* **1999**, *285*, 1811.